THE JOURNAL OF PHYSICAL CHEMISTRY A

ARTICLE

pubs.acs.org/JPCA

Infrared Spectra of Dimethylphenanthrenes in the Gas phase

Prasanta Das, E. Arunan,* and Puspendu K. Das*

Department of Inorganic and Physical Chemistry, Indian Institute of Science, Bangalore 560012, India

Supporting Information

ABSTRACT: Infrared spectra of atmospherically and astronomically important dimethylphenanthrenes (DMPs), namely 1,9-DMP, 2,4-DMP, and 3,9-DMP, were recorded in the gas phase from 400 to 4000 cm^{-1} with a resolution of 0.5 cm^{-1} at 110 °C using a 7.2 m gas cell. DFT calculations at the B3LYP/6-311G** level were carried out to get the harmonic and anharmonic frequencies and their corresponding intensities for the assignment of the observed bands. However, spectral assignments could not be made unambiguously using anharmonic or selectively scaled harmonic frequencies. Therefore, the scaled quantum mechanical (SQM) force field analysis method was adopted to achieve more accurate assignments. In this method force fields instead of frequencies were scaled. The Cartesian force field matrix obtained from the Gaussian calculations was converted to a nonredundant local coordinate force field matrix and then the force fields were scaled to match experimental frequencies in a consistent manner using a modified version of the UMAT program of the QCPE package. Potential energy distributions (PEDs) of the normal modes in terms of nonredundant local coordinates obtained from these calculations helped us derive the nature of the vibration at each frequency. The intensity of observed bands in the experimental spectra was calculated using estimated vapor pressures of the DMPs. An error analysis of the mean deviation between experimental and calculated intensities reveal that the observed methyl C−H stretching intensity deviates more compared to the aromatic C−H and non C−H stretching bands.

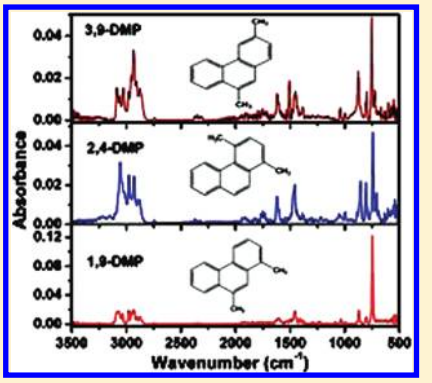

I. INTRODUCTION

Dimethylphenanthrenes are important polycyclic aromatic hydrocarbons (PAHs) that have been identified in interplanetary dust particles (IDPs),[1] carbonaceous chondrite meteorites[2] crude oil,[3] sugar cane soot,[4] and sedimentary rock and coal extracts.[5,6] They are pollutants to the atmosphere[7] and soil,[8] and are known health hazards. Therefore, it is necessary to develop methods for their identification at the molecular level in the presence of other hydrocarbons and organic substances.

Earlier detection of DMPs was done by mass spectrometry in conjunction either with gas chromatography[9] or with a two-step laser desorption/laser ionization.[2] However, no molecular information on them could be obtained from mass spectrometry. Pakdel et al.[10] and Fisher et al.[3] used NMR and IR spectroscopies, respectively, to identify DMPs in hydrocarbon contents from various sources. Molecular identification of various isomers of DMP was not possible by the NMR technique, but low resolution IR (8 cm^{-1}) spectroscopy coupled with a GC enabled identification of the isomers. No detailed spectroscopic information on these important constituents of PAHs were available from such low resolution investigations. Cane et al. recorded the gas phase IR spectra of anthracene and phenanthrene with the help of a heated multipass gas cell.[11,12] The room temperature vapor pressure of phenanthrene is moderate (3.51×10^{-7} atm) and Cane et al. heated the sample to 90 °C to record the IR spectra. They have identified 31 vibrations in the range 500−3200 cm^{-1}. They used the scaled quantum mechanical force field method of Pulay et al.[13] to calculate the spectrum but did not identify the nature of the vibration for the observed fundamentals nor carry out any error analysis of the fitted frequencies. The spectra were noisy and many of the lines were weak. Pirali et al.[14] recorded far-infrared emission spectra of small PAHs including phenanthrene in the gas phase using a liquid helium cooled bolometer detector and recorded the spectra in the 100−700 cm^{-1} range. Density functional theory (DFT) calculation and the tight-binding molecular dynamics (TBMD) simulations were carried out for the assignment of the low frequency vibrations. In this paper we report gas phase infrared spectra of several dimethylphenanthrenes (DMPs) that have not been reported in the literature. The difficulty in recording the gas phase IR spectra of DMPs perhaps lies in the fact that their vapor pressures are lower than that of phenanthrene and it is not easy to get them in appreciable amounts in the gas phase by simple heating. We have used the positive pressure of an inert gas to push enough amounts of DMPs into the heated multipass long-path gas cell. The observed IR frequencies have been assigned by using the scaled force field method used by us earlier[15] at the B3LYP/6-311G** level. In addition, we have done the potential energy distribution of each fundamental vibration in terms of the

Special Issue: A. R. Ravishankara Festschrift

Received: May 16, 2011
Revised: July 10, 2011
Published: July 28, 2011

Table 1. Vapor Pressure of Phenanthrene and DMPs at Room Temperature

compound	state at 25 °C	melting point (in °C)	P (at 25 °C in atm)
phenanthrene	solid powder	100	3.51×10^{-7} [a]
1,9-DMP	solid powder	88	3.80×10^{-8} [b]
2,4-DMP	solid powder	80	3.42×10^{-8} [b]
3,9-DMP	solid powder	62	3.27×10^{-8} [b]

[a] Experimentally measured value at 30 °C.[16] [b] Experimental values for the pressure are not available, and therefore, it was calculated by ACD/Laboratories software found through a SciFinder search.[17]

nonredundant local coordinates which provides a clear picture about the type of motion that is associated with each vibration. We have also done an error analysis to ascertain the correctness of our assignment of the fundamentals.

II. METHODS

A. Experimental Section. Phenanthrene (90%, Fluka) was used as a standard compound for the optimization of our infrared setup and purified by vacuum distillation before use. DMPs chosen in this study are 1,9-dimethylphenanthrene (Chiron, 99.1%), 2,4-dimethylphenanthrene (Chiron, 99.9%), and 3,6-dimethylphenanthrene (Chiron, 99.9% purity), which were obtained commercially and used as received.

DMPs show lower vapor pressures compared to phenanthrene, although they have lower melting points (Table 1). We have used a 7.2 m path length white cell (136G/3TQ, Bruker Optik) equipped with a heating jacket to record the IR spectra. The cell, coupled with a FT-IR spectrometer (Vertex-70, Bruker Optik), was placed vertically to the sample chamber of the spectrometer and aligned with the help of an external HeNe laser. A rotary pump and an argon line were connected to the cell through ball valves. The experimental setup was optimized first with phenanthrene that was heated at 100 °C, and the reported spectrum by Cane et al. was reproduced. Because it was not possible to ensure that the DMP pressure is uniform throughout the cell by heating the whole cell containing a few milligrams of DMP up to 110 °C, Ar gas was used as a carrier. Solid DMP sample was loaded inside a small bulb in the bottom of the cell and the air in the cell was evacuated by pumping. The cell containing DMP was then gently heated above the melting point of the sample and left at 110 °C for 1 h to stabilize the cell body, optics, and other parts of the cell to reach thermal equilibrium. This did not produce enough IR signal to see a good spectrum. Therefore, while heating, ultrahigh purity argon gas was introduced through a ball valve to keep the pressure of the sample uniform throughout the cell. This helped in recording the IR spectrum of these molecules with a good signal-to-noise. Moreover, as pointed out later in section IIC the vapor pressure deduced from the experimental intensities of the various bands are in reasonable agreement with calculated values. The total pressure of argon gas containing DMPs in the cell was maintained at 30 mmHg. Midinfrared spectra (4000−400) cm^{-1} were collected using a liquid nitrogen cooled HgCdTe detector. The spectra were recorded at 0.5 cm^{-1} spectral resolution with averaging over 2048 scans. The total time required for collecting each spectrum was about 1 h. The spectrometer was continuously purged with ultra high purity grade N_2 gas to avoid air contribution to the spectrum. DMPs have low infrared absorbances (Maximum Optical Depth = 0.03) and small amounts of H_2O vapor present inside the cell give rise to infrared absorption bands that overlap with those of DMPs. We have collected the spectra of argon at the experimental pressure and temperature without DMPs separately and subtracted the same from the sample spectra to get H_2O free spectra of the DMPs. In spite of this, in some regions, water peaks interfered with the DMP spectra. The integrated band area $\int \log(I_0/I)\, d\nu$ (in cm^{-1}) for each band was obtained with the help of OPUS software provided by Bruker Optik. Levenberg−Marquardt algorithm in OPUS software was used to calculate single component band area in the region of overlapping bands particularly in the aromatic C−H and methyl C−H stretching regions.

B. Calculation. The quantum-chemical calculations were carried out using density functional theory (DFT). At first the molecular geometry of DMPs were optimized at C_s point group with B3LYP/6-311G** level of theory using Gaussian 2009 program.[18] At the computed equilibrium geometry, harmonic and anharmonic frequencies and their intensities were calculated in a Tesla Cluster (EM64L) system. In the case of 2,4-DMP we found one imaginary frequency due to interaction between an aromatic C−H bond and a methyl group present in the adjacent ring. In this case the optimized structure is a low energy transition state and not the global potential minimum as found for the other two isomers. The internal coordinates of DMPs were defined as individual bond stretching coordinates (r and R), out-of-plane displacements (γ), linear combinations of bond angles (α, β, and ϕ) and torsions (τ) as deformation coordinates, as shown in Figure 1. The numbers of such coordinates are 116, which exceed the number of fundamental vibrations (84). Then a set of nonredundant local coordinates (NLCs) was constructed as recommended by Pulay et al.[13,19] on the basis of linear combinations of the internal coordinates and the symmetry of the molecule. The set of NLCs thus obtained is listed in Table 2. The Gaussian force constant matrix in Cartesian coordinates was then converted to the force constant matrix in NLCs. The force constant matrix was subsequently adjusted to fit the experimentally observed frequencies for the fundamentals using the solution of the inverse eigenvalue equation $\mathbf{GFL} = \mathbf{L}\Lambda$, where $\mathbf{F}$ is the force constant matrix, Λ is the frequency matrix, $\mathbf{G}$ is the Wilson's $\mathbf{G}$ matrix, and $\mathbf{L}$ is the eigenvector matrix describing the normal modes. Normally $\mathbf{F}$ is varied and Λ is calculated until the latter match the experimental frequencies and details of the method described in ref 20. For the observed fundamentals, band origin frequencies are used as input frequencies and for fundamentals that were not observed in experiment, calculated doubly scaled harmonic frequencies are used as inputs in Λ. The force constant matrix is scaled in a consistent and iterative manner to fit Λ. For ab initio calculations it is known that for molecules as small as benzene, at least 1000 iterations are necessary before a good match with the experimental frequencies is obtained.[20] However, in our case, only 100 iterations were enough for calculated harmonic frequencies of such large molecules to match the experimental frequencies. This is one of the advantages of using DFT for fitting the IR spectra of large polyatomic molecules. All these fitting calculations were carried out using the modified UMAT program in the QCPE package.[21,22] We see that the $\mathbf{F}$ matrix in NLC is 82 × 82 dimensional and not 84 × 84 dimensional as expected from the number of NLCs because some of the methyl C−H stretching frequencies are degenerate.

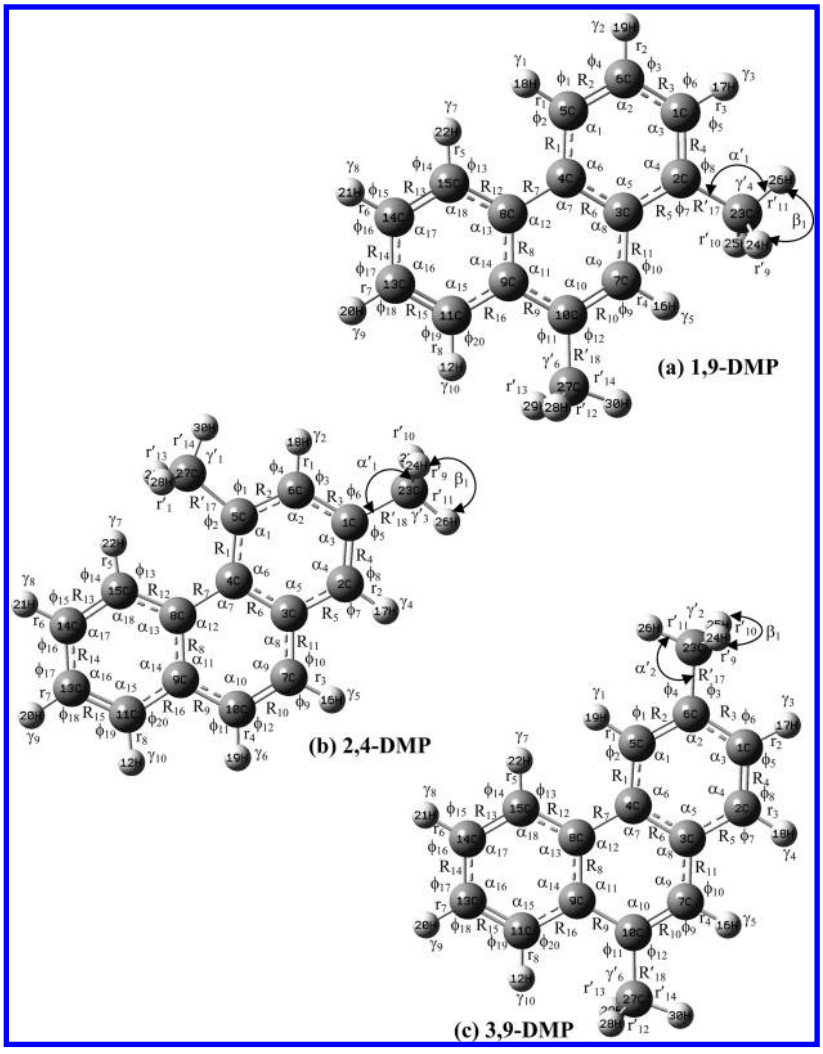

Figure 1. Optimized B3LYP/6-311G** structure and internal coordinates of (a) 1,9-DMP, (b) 2,4-DMP, and (c) 3,9-DMP. Twist coordinates', τ numberings are the same as defined for the C−C bond coordinates (R). α_1' and β_1 are, respectively, the C−C−H and H−C−H angle coordinates of the methyl groups. The other C−C−H and H−C−H angle coordinates, α_2', α_3', etc. and β_2, β_3, etc., respectively, are defined similarly.

In fact, two such frequencies appear degenerate in calculation. In addition, we get the potential energy distributions (PEDs) of the normal modes in terms of the local coordinates, which help us understand the type of vibrational motion associated with the mode. Mean deviations, δ_{freq} (in cm^{-1}) between calculated and observed frequencies for different modes of vibration were evaluated using

$$\delta_{\text{freq}} = \frac{\sum_{i=1}^{n} |\nu_i^{\text{cal}} - \nu_i^{\text{exp}}|}{n} \quad (1)$$

where ν_i^{cal} and ν_i^{exp} are the calculated and observed frequencies, respectively, and n is the total number of observed ca. 30−35 bands.

C. Absolute Intensity Calculation. The absolute intensity from the infrared spectrum can be experimentally determined with good accuracy for small molecules. However, finding the absolute intensity of an IR band from the gas phase IR spectra of large molecules could be challenging if the exact concentration of the molecule is not known, which is applicable for the molecules studied in this paper.

Theoretically integrated infrared band intensities (km mol^{-1}) were calculated employing the formula[23]

$$A_i^{\text{cal}} = 42.254 \left| \frac{\partial \mu}{\partial Q_i} \right|^2 \quad (2)$$

where $\partial\mu/\partial Q_i$ are the dipole moment derivatives in D (Å $\text{amu}^{1/2}$) evaluated via analytical derivatives computed at the DFT level. Experimentally absolute intensities (cm^{-2} atm^{-1}) were calculated using[24]

$$A_i^{\text{exp}} = \frac{2.303 \int \log(I_0/I)_i \, d\nu_i}{P_i l} \quad (3)$$

where l (in cm) is the optical path length and P_i's (in atm) are the vapor pressures. In our experiment, it is not possible to get the vapor pressure of DMPs by conventional pressure measurement because they are seeded with an excess of argon. Therefore, we estimate the vapor pressures (P_i's) by using A_i^{cal} obtained from calculation instead of A_i^{exp} in eq 3. The average pressure obtained from all the bands were then calculated using $P = \sum_{i=1}^{n} P_i/n$, where

dx.doi.org/10.1021/jp2045542 |J. Phys. Chem. A 2012, 116, 5769–5778

Table 2. Nonredundant Local Coordinates of DMPs

compound	nonredundant local coordinates	designation	description
1,9-DMP[a]	in-plane		
	$S_{1-16} = R_i$	R_{1-16}	Ar, C−C stretch
	$S_{20,22} = R'_i$	$R'_{17,18}$	Ar−CH_3,C−C stretch
	$S_{17-19,21,23-26} = r_i$	r_{1-8}	Ar, C−H stretch
	$S_{27-32} = r'_i$	r'_{9-14}	CH_3, C−H stretch
	$S_{33-35,37,39-42} = 2^{-1/2}(\phi_3 - \phi_4); (\phi_7 - \phi_8)...$	$\beta_{1-3,5,7-10}$	Ar, C−H def
	$S_{36,38} = 2^{-1/2}(\phi_1 - \phi_2); (\phi_5 - \phi_6)$	$\beta'_{4,6}$	C−CH_3, C−C def
	$S_{43,46,49} = 6^{-1/2}(\alpha_1 - \alpha_2 + \alpha_3 - \alpha_4 + \alpha_5 - \alpha_6)$	$\delta_1, \delta_4, \delta_7$	ring def
	$S_{44,47,50} = 12^{-1/2}(2\alpha_1 - \alpha_2 - \alpha_3 + 2\alpha_4 - \alpha_5 - \alpha_6)$	$\delta_2, \delta_5, \delta_8$	ring def
	$S_{45,48,51} = 1/2(\alpha_2 + \alpha_3 - \alpha_5 - \alpha_6)$	$\delta_3, \delta_6, \delta_9$	ring def
	out-of-plane		
	$S_{52,57} = 6^{-1/2}(\alpha'_1 + \alpha'_2 + \alpha'_3 - \beta_1 - \beta_2 - \beta_3)$	$\delta_a(1), \delta_a(2)$	CH_3 sym def
	$S_{53,58} = 6^{-1/2}(2\alpha'_1 - \alpha'_2 - \alpha'_3)$	$\delta_s(1), \delta_s(2)$	CH_3 asym def
	$S_{54,59} = 2^{-1/2}(\alpha'_2 - \alpha'_3)$	$\delta_s(1), \delta_s(2)$	CH_3 asym def
	$S_{55,60} = 6^{-1/2}(2\beta_1 - \beta_2 - \beta_3)$	$\rho(1), \rho(2)$	CH_3 rocking
	$S_{56,61} = 2^{-1/2}(\beta_2 - \beta_3)$	$\rho(1), \rho(2)$	CH_3 rocking
	$S_{62,64,65,68-71} = \gamma_i$	$\gamma_{1-3,5,7-10}$	Ar, C−H wag
	$S_{65,67} = \gamma'_i$	$\gamma'_{4,6}$	Ar−CH_3, C−C wag
	$S_{72,75,78} = 6^{-1/2}(\tau_1 - \tau_2 + \tau_3 - \tau_4 + \tau_5 - \tau_6)$	τ_1, τ_4, τ_7	ring torsion
	$S_{73,76,79} = 1/2(\tau_1 - \tau_3 + \tau_4 - \tau_6)$	τ_2, τ_5, τ_8	ring torsion
	$S_{74,77,80} = 12^{-1/2}(-\tau_1 + 2\tau_2 - \tau_3 - \tau_4 + 2\tau_5 - \tau_6)$	τ_3, τ_6, τ_9	ring torsion
	$S_{81} = 2^{-1/2}(\tau_{5-4-3-7} - \tau_{8-4-3-2})$	τ_{ring}	ring torsion
	$S_{82} = 2^{-1/2}(\tau_{4-8-9-11} - \tau_{15-8-9-10})$	τ_{ring}	ring torsion
	$S_{83,84} = \tau_{2-23}; \tau_{10-17}$	$\tau''_{17,18}$	Ar−CH_3, C−C twist
2,4-DMP[a]	in-plane		
	$S_{1-16} = R_i$	R_{1-16}	Ar, C−C stretch
	$S_{17,19} = R'_i$	$R'_{17,18}$	Ar−CH_3, C−C stretch
	$S_{18,22-26} = r_i$	r_{1-8}	Ar, C−H stretch
	$S_{27-32} = r'_i$	r'_{9-14}	CH_3, C−H stretch
	$S_{33,35} = 2^{-1/2}(\phi_1 - \phi_2); (\phi_5 - \phi_6)\ (\beta'_i)$	$\beta'_{1,3}$	C−CH_3 def
	$S_{34,36-42} = 2^{-1/2}(\phi_3 - \phi_4); (\phi_7 - \phi_8)...\ (\beta_i)$	$\beta_{2,4-10}$	Ar, C−H def
	$S_{43,46,49} = 6^{-1/2}(\alpha_1 - \alpha_2 + \alpha_3 - \alpha_4 + \alpha_5 - \alpha_6)$	$\delta_1, \delta_4, \delta_7$	ring def
	$S_{44,47,50} = 12^{-1/2}(2\alpha_1 - \alpha_2 - \alpha_3 + 2\alpha_4 - \alpha_5 - \alpha_6)$	$\delta_2, \delta_5, \delta_8$	ring def
	$S_{45,48,51} = 1/2(\alpha_2 + \alpha_3 - \alpha_5 - \alpha_6)$	$\delta_3, \delta_6, \delta_9$	ring def
	out-of-plane		
	$S_{52,57} = 6^{-1/2}(\alpha'_1 + \alpha'_2 + \alpha'_3 - \beta_1 - \beta_2 - \beta_3)$	$\delta_a(1), \delta_a(2)$	CH_3 sym def
	$S_{53,58} = 6^{-1/2}(2\alpha'_1 - \alpha'_2 - \alpha'_3)$	$\delta_s(1), \delta_s(2)$	CH_3 asym def
	$S_{54,59} = 2^{-1/2}(\alpha'_2 - \alpha'_3)$	$\delta_s(1), \delta_s(2)$	CH_3 asym def
	$S_{55,60} = 6^{-1/2}(2\beta_1 - \beta_2 - \beta_3)$	$\rho(1), \rho(2)$	CH_3 rock
	$S_{56,61} = 2^{-1/2}(\beta_2 - \beta_3)$	$\rho(1), \rho(2)$	CH_3 rock
	$S_{62,64} = \gamma'_i$	$\gamma'_{1,3}$	Ar−CH_3, C−C wag
	$S_{63,65-71} = \gamma_i$	$\gamma_{2,4-10}$	Ar, C−H wag
	$S_{72,75,78} = 6^{-1/2}(\tau_1 - \tau_2 + \tau_3 - \tau_4 + \tau_5 - \tau_6)$	τ_1, τ_4, τ_7	ring torsion
	$S_{73,76,79} = 1/2(\tau_1 - \tau_3 + \tau_4 - \tau_6)$	τ_2, τ_5, τ_8	ring torsion
	$S_{74,77,80} = 12^{-1/2}(-\tau_1 + 2\tau_2 - \tau_3 - \tau_4 + 2\tau_5 - \tau_6)$	τ_3, τ_6, τ_9	ring torsion
	$S_{81} = 2^{-1/2}(\tau_{5-4-3-7} - \tau_{8-4-3-2})$	τ_{ring}	ring torsion
	$S_{82} = 2^{-1/2}(\tau_{4-8-9-11} - \tau_{15-8-9-10})$	τ_{ring}	ring torsion
	$S_{83,84} = \tau_{1-23}; \tau_{5-27}\ (\tau''_i)$	$\tau''_{17,18}$	Ar−CH_3, C−C twist
3,9-DMP[a]	in-plane		
	$S_{1-16} = R_i$	R_{1-16}	Ar, C−C stretch
	$S_{18,22} = R'_i$	$R'_{17,18}$	Ar−CH_3,C−C stretch
	$S_{17,19-21,23-26} = r_i$	r_{1-8}	Ar, C−H stretch
	$S_{27-32} = r'_i$	r'_{9-14}	CH_3, C−H stretch
	$S_{33,35-37,39-42} = 2^{-1/2}(\phi_3 - \phi_4); (\phi_7 - \phi_8)...$	$\beta_{1,3-5,7-10}$	Ar, C−H def

dx.doi.org/10.1021/jp2045542 |J. Phys. Chem. A 2012, 116, 5769–5778

Table 2. Continued

compound	nonredundant local coordinates	designation	description
	$S_{34,38} = 2^{-1/2}(\phi_1 - \phi_2)$; $(\phi_5 - \phi_6)$	$\beta'_{2,6}$	C−CH_3 def
	$S_{43,46,49} = 6^{-1/2}(\alpha_1 - \alpha_2 + \alpha_3 - \alpha_4 + \alpha_5 - \alpha_6)$	$\delta_1, \delta_4, \delta_7$	ring def
	$S_{44,47,50} = 12^{-1/2}(2\alpha_1 - \alpha_2 - \alpha_3 + 2\alpha_4 - \alpha_5 - \alpha_6)$	$\delta_2, \delta_5, \delta_8$	ring def
	$S_{45,48,51} = 1/2(\alpha_2 + \alpha_3 - \alpha_5 - \alpha_6)$	$\delta_3, \delta_6, \delta_9$	ring def
	out-of-plane		
	$S_{52,57} = 6^{-1/2}(\alpha'_1 + \alpha'_2 + \alpha'_3 - \beta_1 - \beta_2 - \beta_3)$	$\delta_a(1), \delta_a(2)$	CH_3 sym def
	$S_{53,58} = 6^{-1/2}(2\alpha'_1 - \alpha'_2 - \alpha'_3)$	$\delta_s(1), \delta_s(2)$	CH_3 asym def
	$S_{54,59} = 2^{-1/2}(\alpha'_2 - \alpha'_3)$	$\delta_s(1), \delta_s(2)$	CH_3 asym def
	$S_{55,60} = 6^{-1/2}(2\beta_1 - \beta_2 - \beta_3)$	$\rho(1), \rho(2)$	CH_3 rock
	$S_{56,61} = 2^{-1/2}(\beta_2 - \beta_3)$	$\rho(1), \rho(2)$	CH_3 rock
	$S_{62,64-66,69-71} = \gamma_i$	$\gamma_{1,3-5,7-10}$	Ar, C−H wag
	$S_{63,68} = \gamma'_i$	$\gamma'_{2,6}$	Ar−CH_3, C−C wag
	$S_{72,75,78} = 6^{-1/2}(\tau_1 - \tau_2 + \tau_3 - \tau_4 + \tau_5 - \tau_6)$	τ_1, τ_4, τ_7	ring torsion
	$S_{73,76,79} = 1/2(\tau_1 - \tau_3 + \tau_4 - \tau_6)$ (τ_2, τ_5, τ_8)	τ_2, τ_5, τ_8	ring torsion
	$S_{74,77,80} = 12^{-1/2}(-\tau_1 + 2\tau_2 - \tau_3 - \tau_4 + 2\tau_5 - \tau_6)$	τ_3, τ_6, τ_9	ring torsion
	$S_{81} = 2^{-1/2}(\tau_{5-4-3-7} - \tau_{8-4-3-2})$	τ_{ring}	ring torsion
	$S_{82} = 2^{-1/2}(\tau_{4-8-9-11} - \tau_{15-8-9-10})$	τ_{ring}	ring torsion
	$S_{83,84} = \tau_{6-23}$; τ_{10-27}	$\tau''_{17,18}$	Ar−CH_3, C−C twist

[a] All internal coordinates are according to Figure 1a−c for 1,9-, 2,4-, and 3,9-DMP, respectively. Ar refers to aromatic.

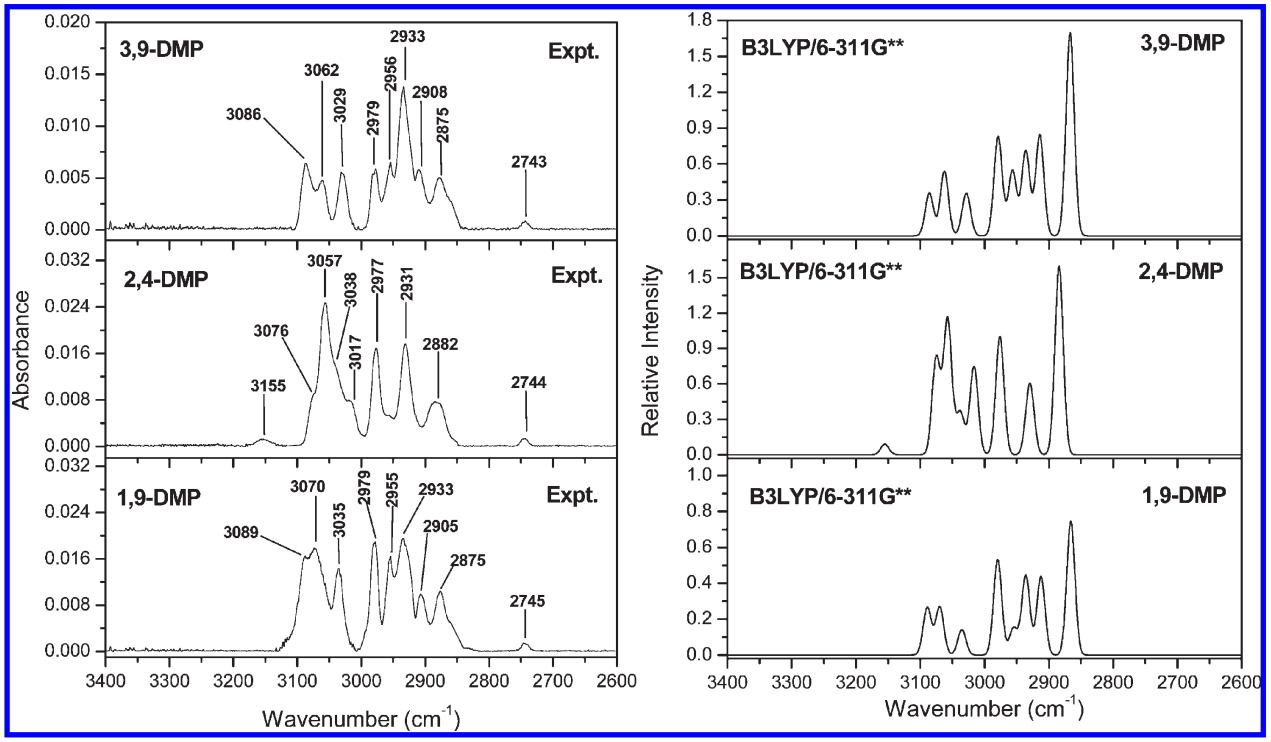

Figure 2. Observed gas phase IR absorption spectra and calculated spectra of 1,9-, 2,4-, and 3,9-DMPs from 3400 to 2600 cm^{-1} at 0.5 cm^{-1} spectral resolution. Relative intensities are obtained with respect to the intense band at ∼750 cm^{-1}.

n is the number of observed bands. The average pressure is then put back into eq 3 to get A_i^{exp}, that is, the absolute intensity of the band. The average vapor pressures found to be $(1.07 \pm 0.73) \times 10^{-5}$, $(0.91 \pm 0.75) \times 10^{-5}$, and $(0.53 \pm 0.51) \times 10^{-5}$ atm for 1,9-, 2,4-, and 3,9-DMP, respectively, when B3LYP/6-311G** calculated intensities were used for the vapor pressure calculation. Our estimated vapor pressures at 110 °C are 3 orders of magnitude higher compared to the ACD predicted vapor pressures at 25 °C (Table 1). This increase in vapor pressure is due to an increase of temperature by 85 °C. For example, the ACD predicted vapor pressure for 9,10-DMP is 2.43×10^{-8} atm at 25 °C whereas at 110 °C it is calculated to be 2.85×10^{-5} atm using the Antoine equation.[25] It implies that the ACD predicted vapor pressures listed in Table 1 are reasonable and our estimated vapor pressures from experimental spectra are consistent with that estimation. To convert the experimental

dx.doi.org/10.1021/jp2045542 |J. Phys. Chem. A 2012, 116, 5769–5778

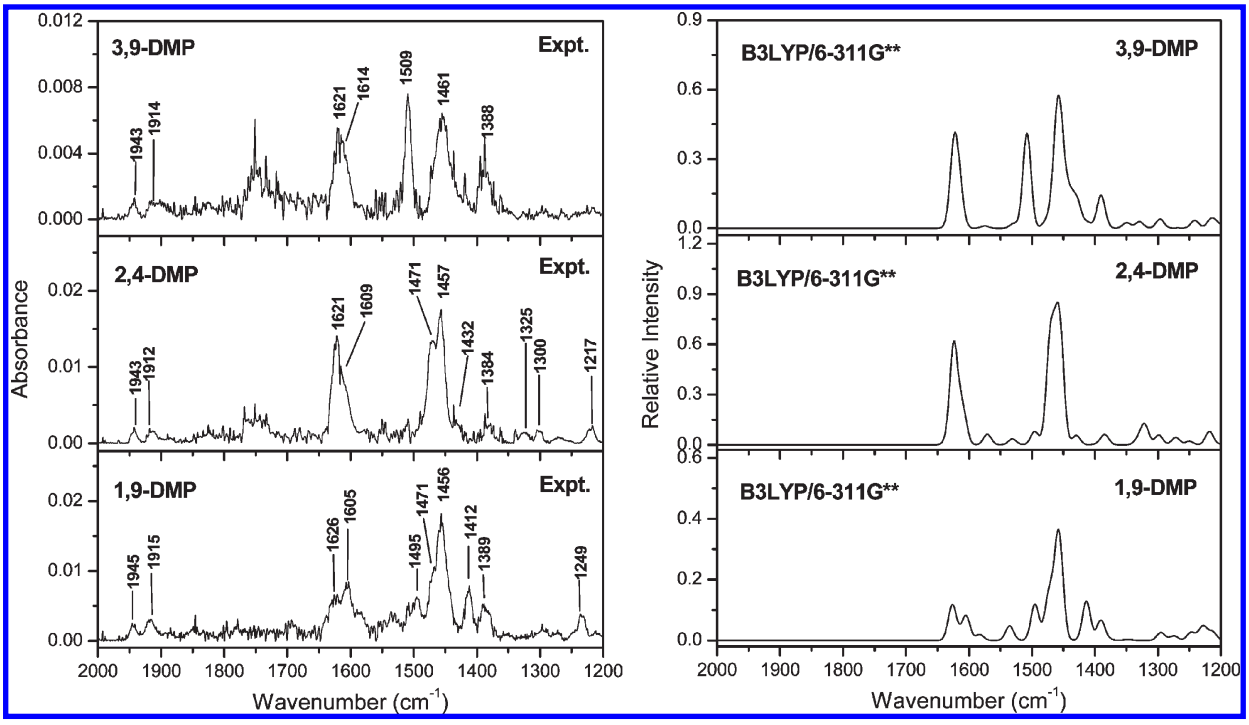

Figure 3. Observed gas phase IR absorption spectra and calculated spectra of 1,9-, 2,4-, and 3,9-DMPs from 2000 to 1200 cm^{-1} at 0.5 cm^{-1} spectral resolution. Relative intensities were obtained with respect to the intense band at ~750 cm^{-1}.

intensities in km mol^{-1}, the values in cm^{-2} atm^{-1} were multiplied by a factor of 82.056 (T/K). Observed band area (cm^{-1}), calculated intensity (km mol^{-1}), vapor pressure of individual bands (atm), and the observed band intensity (km mol^{-1}) for all the bands are presented in the Supporting Information. The mean deviations between calculated and observed band intensities for different modes of vibration were evaluated by

$$\delta_{\text{int}} = \frac{\sum_{i=1}^{n} |A_i^{\text{cal}} - A_i^{\text{exp}}|}{n} \quad (4)$$

where A_i^{cal} and A_i^{exp} are the calculated and experimental intensities and n is the total number of observed bands.

III. RESULTS AND DISCUSSION

The gas phase IR absorption spectra and calculated spectra of DMPs are shown in Figures 2−4. The normal modes of the DMP molecule in C_s symmetry belong to the irreducible representation (55A′ + 29A″). We have observed 30−35 bands. The only gas phase IR spectrum for DMPs that is listed in the NIST IR spectral library is that of 3,6-DMP at low resolution and only 21 bands are seen in the spectrum. In our study, the experimental band-origin frequencies and their intensities, calculated harmonic, anharmonic, and scaled force field fitted frequencies, intensities and their corresponding PEDs are tabulated in the Supporting Information. For generating the calculated spectra, force field fitted frequencies were used and fwhm of the bands were assumed to be 15 cm^{-1}, which is based on the observed bandwidth of the most intense band around 750 cm^{-1}. Table 3 lists the mean deviation between the calculated and observed frequencies in the DMPs. It is clear from the table that the extent of anharmonicity is different for the three different classes of vibration such as aromatic C−H stretching, methyl C−H stretching, etc. listed in the table. It is also apparent that the agreement between the force field fitted and observed frequencies are very good and are within a few cm^{-1}. Table 4 lists the mean deviation between the calculated and observed band intensities for the three different classes of vibration. It is clear that the intense vibrations in the experimental spectra are also intense in the calculated spectra except for the bands in the methyl C−H stretching region.

The observed spectra of DMPs have been divided into four distinct regions: (1) 3200−2800 cm^{-1} for aromatic C−H and methyl C−H stretching; (2) 1700−1200 cm^{-1} for aromatic C−C stretching, methyl C−H symmetric and asymmetric deformations, in-plane aromatic ring deformation, etc.; (3) 1200−500 cm^{-1} for aromatic C−H out-of-plane vibration and out-of-plane aromatic ring deformation, etc.; (4) 2800−1800 cm^{-1} for nonfundamental vibrations such as overtone and combination bands. Details of the assignment have been discussed regionwise in the following section.

A. Spectral Region 3200−2800 cm^{-1}. Two types of bands appear in this region. They are aromatic C−H and methyl C−H stretching vibrations. The assignment of the observed bands in this region is always difficult because of the presence of Fermi resonances.[26] In the aromatic C−H stretching region, Fermi resonances occur due to the interaction of a fundamental mode with a lower frequency overtone or combination mode, whereas, in the methyl C−H stretching region, they generally occur due to the interaction between the methyl C−H symmetric stretch and an overtone involving two quanta of a methyl deformation mode. Due to Fermi resonances the intensity of the bands that result from the interaction change the original intensity of the band and more spectral lines are observed than expected. In our case, we cannot rule out the presence of Fermi resonances in this region of the spectrum and, thus, our assignment with the help of force fitted frequencies is tentative.

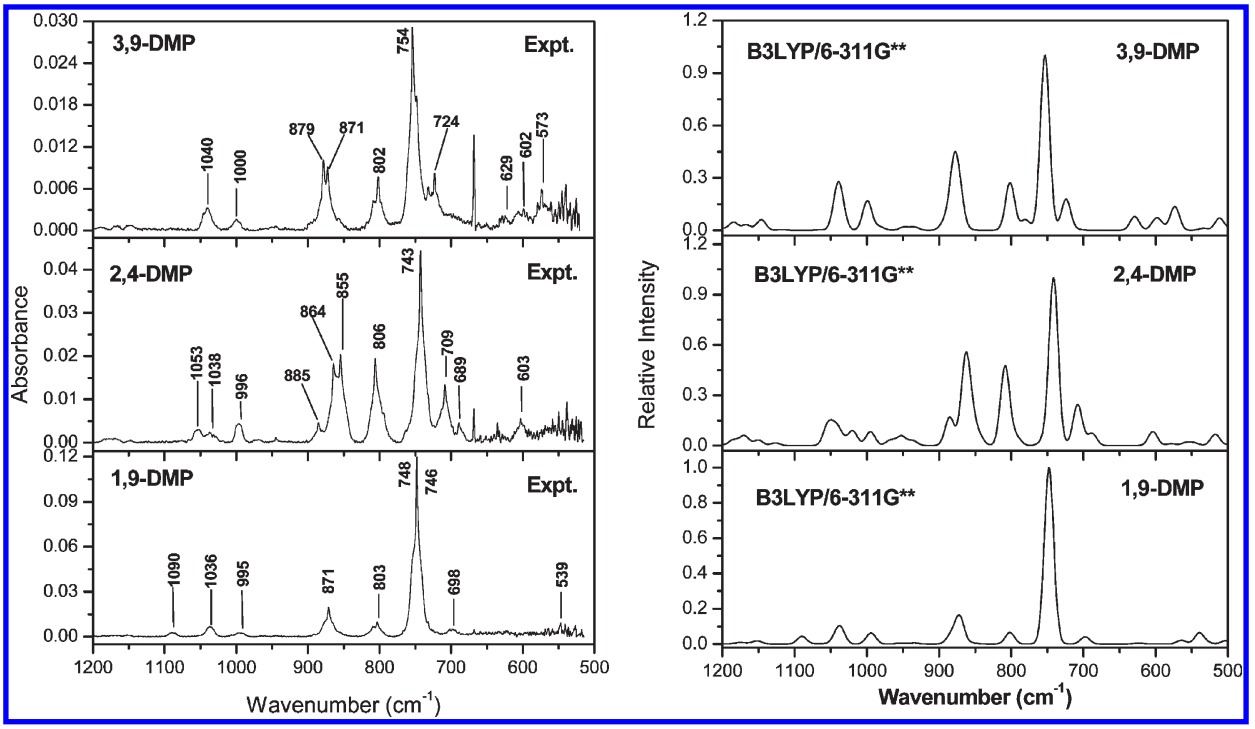

Figure 4. Observed gas phase IR absorption spectra and calculated spectra of 1,9-, 2,4-, and 3,9-DMPs from 1200 to 500 cm^{-1} at 0.5 cm^{-1} spectral resolution. The relative intensities are obtained with respect to the intense band at ~750 cm^{-1}.

Table 3. Mean Deviation, δ_{freq} (cm^{-1}), between Calculated Anharmonic and Fitted Frequencies from Observed Frequencies

	anharmonic			fitted		
δ_{freq}/mode of vibration	1,9-DMP	2,4-DMP	3,9-DMP	1,9-DMP	2,4-DMP	3,9-DMP
aromatic C−H stretching	36.8	20.0	36.8	<0.1	0.7	<0.1
methyl C−H stretching	23.5	13.8	23.5	6.4	1.0	6.4
non C−H stretching	8.6	8.0	8.6	0.8	1.7	0.8

A group of five bands observed at 3089.1, 3069.7, 3035.3, 2979.6, and 2955.2 cm^{-1} in 1,9-DMP; 3155.1, 3076.5, 3057.2, 3038.0, and 3017.1 cm^{-1} in 2,4-DMP; and 3085.7, 3062.5, 3029.1, 2978.9, and 2956.3 cm^{-1} in 3,9-DMP match well with the scaled force field frequencies at 3089.1, 3069.8, 3035.3, 2979.8, and 2955.2 cm^{-1} in 1,9- DMP; 3155.1, 3075.2, 3057.7, 3039.3, and 3018.1 cm^{-1} in 2,4-DMP; and 3085.8, 3062.5, 3030.6, 2978.9, and 2957.0 cm^{-1} in 3,9-DMP, respectively (Figure 2). These bands are assigned to aromatic C−H stretching vibrations. In phenanthrene and 1-methylphenanthrene only one broad band has been observed in this region.[27] The methyl group substitution at two different positions in phenanthrene increases the local charge distribution around the CH bonds and thus more spectral lines are visible in the spectrum.

A group of three bands of the methyl C−H stretching vibration is seen in the experimental spectra of all the DMPs. Out of these three bands two bands at 2933.5 and 2905.0 cm^{-1} in 1,9-DMP; 2976.7 and 2930.8 cm^{-1} in 2,4-DMP; and 2933.5 and 2908.2 cm^{-1} in 3,9-DMP correspond to the methyl asymmetric C−H stretching. The other band at a lower frequency of 2875.3, 2882.3, and 2875.0 cm^{-1} for 1,9-, 2,4-, and 3,9-DMP, respectively, is due to methyl symmetric C−H stretching. This band is of low absolute intensity in 1,9-DMP and of moderate intensity in the other two isomers. From the frequency and intensity tables (Supporting Information) it appears that the anharmonic frequencies of the antisymmetric/symmetric methyl C−H stretching vibrations are either overestimated or underestimated in the calculations.

Table 4. Mean Deviation, δ_{int} (km mol^{-1}), between B3LYP/6-311G Calculated and Observed Intensity of Different Modes of Vibration in DMPs**

δ_{int}/mode of vibration	1,9-DMP	2,4-DMP	3,9-DMP
aromatic C−H stretching	3.96	13.48	12.81
methyl C−H stretching	31.63	24.19	35.89
non C−H stretching	2.92	2.12	2.90

The absolute intensity of C−H stretching bands does not match well with calculation and the mean deviations found to be 10−30 km mol^{-1} for the three DMPs dealt here. Cavagnat et al. observed three bands at 2882.0, 2935.0, and 3005.0 cm^{-1} for a small molecule like toluene and assigned them to a methyl C−H stretching vibration.[26e] In toluene these bands mismatch by 15−30 cm^{-1} from the calculated frequencies and they have proposed that this deviation is due to the strong Fermi resonance.

dx.doi.org/10.1021/jp2045542 |J. Phys. Chem. A 2012, 116, 5769–5778

From Table 3 it is clear that the observed frequencies deviate by ~20 cm^{-1} with respect to the calculated anharmonic frequencies of DMPs. In addition, the deviation of methyl C−H stretching band intensity (Table 4) from the calculated one is larger compared to those of the aromatic C−H stretching frequencies. This large deviation may be due to the occurrence of Fermi resonances between the methyl C−H stretch and two quanta of methyl deformation vibrations observed at ~1470 cm^{-1}. It is difficult to confirm such kind resonances for large molecules like DMPs because the number of calculated frequencies is higher compared to the number of observed bands in the C−H stretch region. Another feature in calculation that has been noticed in the methyl C−H stretching region, is the interchange of PEDs in some instances. When two frequencies are close, their PEDs get mixed-up but in our case they do not change the assignment because the number of observed bands in the methyl C−H stretch regions are only three and they are well-separated.

B. Spectral Region 1700−1200 cm^{-1}. Several bands have been identified in this region, and they belong to the A′ irreducible representation. We could assign the bands in this region after subtracting the H_2O spectrum because they interfere with the bands of DMPs in this region. Bands observed at 1626.5 and 1604.6 cm^{-1} in 1,9-DMP, 1621.4 and 1609.1 cm^{-1} in 2,4-DMP, and 1620.8 and 1614.2 cm^{-1} in 3,9-DMP are assigned to aromatic C−C stretching vibrations from the PEDs (Figure 3). These bands have low intensities in 1,9-DMP and moderate intensities in 2,4- and 3,9-DMPs although some of them are not very well-resolved.

The absolute intensities of the bands in this region are larger compared to those in phenanthrene,[12] which has to perhaps do with methyl substitution in the DMPs. In phenanthrene π-electron localization occurs and all the C−C bonds are not of equal length.[28] The C−C bond lengths will change further with methyl substitutions depending on where they are made.[29] This will affect the charge distributions on the aromatic carbon atoms which will alter the C−C bond dipole moments. In 2,4-DMP the atomic polar tensor (APT) charges on carbon atoms 1, 2, 5, and 6 are +0.124e, −0.106e, +0.044e, and −0.122e, respectively, whereas in phenanthrene corresponding charges are −0.039e, −0.004e, −0.056e, and −0.036e (Supporting Information). It is clear that methyl substitution makes the C−C bonds more polar compared to C−C bonds in unsubstituted phenanthrene. This leads to larger change in dipole moments for C−C stretches in DMPs compared to those in phenanthrene. This is why the C−C stretching modes in DMPs are more intense compared to those in phenanthrene.

A low intensity band found at 1495.4 cm^{-1} in 1,9-DMP is correlated with the force field fitted frequency at 1495.3 cm^{-1} whereas in 3,9-DMP, another moderate intensity band seen at 1508.8 cm^{-1} corresponds to the force field fitted frequency of 1507.9 cm^{-1}. This band is assigned to aromatic C−C stretching vibration (R) in 1,9-DMP and aromatic C−H in-plane bending (β) vibration in 3,9-DMP, as seen from their PEDs. A pair of bands seen at 1471.2 and 1456.0 cm^{-1} in 1,9-DMP; 1470.9 and 1457.4 cm^{-1} in 2,4-DMP; and 1460.6 and 1453.5 cm^{-1} in 3,9-DMP have been assigned to methyl C−H antisymmetric deformation vibrations (δ_s). We could not measure individual band intensity in this region because bands are not well-separated in the recorded spectra. However, the total intensity of the observed bands is comparable to the sum of the calculated individual band intensities between the different DMP isomers.

A low intensity band observed at 1412.4 cm^{-1} in 1,9-DMP and at 1431.8 cm^{-1} in 2,4-DMP has been assigned to aromatic C−H in-plane bending vibration (β) by comparing with the scaled force field fitted frequencies at 1413.5 cm^{-1} in 1,9-DMP and 1429.6 cm^{-1} in 2,4-DMP, respectively. This band is not observed in 3,9-DMP. Perhaps it has been masked by the strong methyl C−H antisymmetric deformation vibration at 1460.6 cm^{-1}. The next low intensity band observed at 1389.5, 1384.4, and 1388.3 cm^{-1} for 1,9-DMP, 2,4-DMP, and 3,9-DMP, respectively, is unique and is assigned to a mixture of in-plane aromatic ring deformation (δ) and out-of-plane methyl rocking vibration (ρ) in 1,9-DMP, out-of-plane methyl rocking vibration (ρ) in 2,4-DMP, and a mixture of out-of-plane methyl rocking (ρ) and aromatic C−C stretching vibrations (R) in 3,9-DMP. A low intensity band found in the region 1213.0−1217.0 cm^{-1} is assigned to either aromatic C−C stretching vibration (R) or aromatic C−H in-plane bending vibration (β) using PEDs. The absolute intensities of the observed bands match well with the calculated ones with a mean deviation of ~4 km mol^{-1}, which is less compared to that for the aromatic C−H and methyl C−H stretching bands.

C. Spectral Region 1200−500 cm^{-1}. Bands observed in this region belong to both the A′ and A″ irreducible representations. The band observed at 1185.0 cm^{-1} in 3,9-DMP (Figure 4) is assigned to a mixture of aromatic-methyl C−C stretching (R′) and aromatic C−C stretching (R) vibrations by comparing with the force field fitted frequency at 1184.9 cm^{-1}. This band is of low intensity and is not observed in the rest of the isomers of DMP. A band observed at 1152.7 cm^{-1} in 1,9-DMP, at 1148.6 cm^{-1} in 2,4-DMP, and at 1150.0 cm^{-1} in 3,9-DMP is of low intensity and is assigned to the aromatic C−C stretching vibration (R) in 1,9-DMP, the aromatic C−H in-plane bending vibrations (β) in 2,4-DMP, and a mixture of aromatic methyl C−C stretching (R′) and aromatic C−H in-plane-bending vibrations (β) in 3,9-DMP. Another weak band observed at 1036.4 cm^{-1} in 1,9-DMP, 1053.2 cm^{-1} in 2,4-DMP, and 1040.4 cm^{-1} in 3,9-DMP is correlated with the scaled frequency at 1036.5 cm^{-1} in 1,9-DMP, 1053.9 cm^{-1} in 2,4-DMP, and 1040.8 cm^{-1} in 3,9-DMP, respectively. This band is assigned as an aromatic C−C stretching vibration (R) in 1,9- and 2,4-DMP and a mixture of aromatic C−C stretching (R) and aromatic ring deformation vibrations (δ) in 3,9-DMP.

A low intensity band observed at 885.3 cm^{-1} in 2,4-DMP is assigned to a mixture of methyl rocking (ρ) and aromatic C−H out-of-plane (γ) vibrations by comparing with the scaled force field fitted frequency at 885.3 cm^{-1}. A moderately intense band observed at 871.4 cm^{-1} in 1,9-DMP is assigned to aromatic C−H out-of-plane bending vibration (γ). On the other hand, in 2,4- and 3,9-DMP this band appears as a doublet at 864.2 and 855.0 cm^{-1} and at 879.1 and 871.7 cm^{-1}, respectively, due to a coupled local coordinate vibration of the aromatic C−H out-of-plane bending (γ) and methyl rocking (ρ) modes. A highly intense band observed at 748.3/746.0 cm^{-1} in 1,9-DMP, 742.7 cm^{-1} in 2,4-DMP, and 753.9 cm^{-1} in 3,9-DMP corresponds to the force field fitted band at 749.0/746.7 cm^{-1} in 1,9-DMP, 741.4 cm^{-1} in 2,4-DMP, and 753.4 cm^{-1} in 3,9-DMP, respectively, which is assigned to the aromatic C−H out-of-plane bending (γ) vibration. In these regions three bands have been found experimentally at 730, 806, and 860 cm^{-1} in phenanthrene and 744, 799, and 876 cm^{-1} in 1-methylphenanthrene.[27] They have been wrongly assigned as a pure aromatic C−H out-of-plane bending vibration. The PEDs in DMPs reveal that these bands are not only responsible for the aromatic C−H out-of-plane bending vibrations but also a mixture of local coordinate vibrations, like methyl rocking and aromatic ring torsion

Table 5. Comparison of the Observed and Calculated Anharmonic and Force Field Fitted Nonfundamental Frequencies (cm^{-1}) of DMPs

	observed		anharmonic	fitted	assignment	
compound	freq	int[a]	6-311G**	6-311G**	overtone	combination
1,9-DMP	1915.5	2.37	1922.4	1908.0		$\nu_{66} + \nu_{40}$
	1944.8	1.18	2078.8/1979.8	2073.0/1961.4	$2\nu_{40}$	$/\nu_{66} + \nu_{37}$
	2745.5	1.18	2751.0/2753.3	2781.2/2750.9	$2\nu_{24}$	$/\nu_{29} + \nu_{21}$
2,4-DMP	1912.5	2.05	1952.9	1916.9		$\nu_{66} + \nu_{38}$
	1943.1	1.66	1989.0/2028.0	1990.2/1958.8	$2\nu_{41}$	$/\nu_{68} + \nu_{36}$
	2744.4	1.56	2896.6/2762.7	2908.8/2758.8	$2\nu_{21}$	$/\nu_{29} + \nu_{20}$
3,9-DMP	1913.8	3.91	1931.5	1919.9		$\nu_{65} + \nu_{39}$
	1942.9	2.61	2096.0/1966.5	2081.6/1947.9	$2\nu_{39}$	$/\nu_{68} + \nu_{36}$
	2743.5	2.39	2774.7/2771.0	2781.6/2757.4	$2\nu_{24}$	$/\nu_{29} + \nu_{20}$

[a] Absolute intensities are in km mol^{-1}.

vibrations. Intense C−H out-of-plane bending frequency is shifted by 14 cm^{-1} in 1-methylphenanthrene and 12−24 cm^{-1} in DMPs with respect to that in phenanthrene. The positive frequency shift and decrease in intensity of the C−H out-of-plane bending mode in mono- and disubstituted benzenes were well documented by Kross et al.[30] on the basis of the theory of orbital rehybridization. They stated that "in aromatic C−H out-of-plane bending vibrations, the bonding orbital of the carbon atom tends to follow the direction of the H-atom moment. The more the carbon bonding orbital is able to follow the moment of the hydrogen atom by changing its hybridization more easily vibrations will occur and vibration frequencies decrease. In benzenoid systems this tendency is a maximum in compounds having a maximum π-electron density associated with the ring." With a weak electron donating methyl group the tendency of the bonding orbital to follow the attached hydrogen is weakened and the aromatic C−H out-of-plane bending vibration moves to higher frequency as found in the case of DMPs. A low intensity band observed at 698.5 cm^{-1} in 1,9-DMP, 688.7 cm^{-1} in 2,4-DMP, and 629.1 cm^{-1} in 3,9-DMP is assigned to the in-plane aromatic ring deformation vibration (δ). This vibration appears at 617 cm^{-1} in phenanthrene spectrum.[14] Bands observed in the lower frequency region such as at 603.2 cm^{-1} in 2,4-DMP and at 602.1 cm^{-1} in 3,9-DMP are assigned to a mixture of torsion around aromatic C−C bond (τ) and aromatic C−H out-of-plane bend (γ) vibrations. In this region too the observed band intensities deviate by 4 km mol^{-1} from the calculated ones, which is similar to what is observed in the 2000−1200 cm^{-1} region.

D. Nonfundamental Bands. A number of bands appear in the spectrum, which do not correspond to any calculated fundamentals, are assigned as combination or overtone bands (Table 5). Initially, nonfundamental bands are tentatively assigned using calculated anharmonic frequencies at the B3LYP/6-311G** level. The band observed at 1915.5 cm^{-1} in 1,9-DMP, 1912.5 cm^{-1} in 2,4-DMP, and 1913.8 cm^{-1} in 3,9-DMP can be correlated with the calculated anharmonic band at 1922.4 cm^{-1} in 1,9-DMP, 1952.9 cm^{-1} in 2,4-DMP, and 1931.5 cm^{-1} in 3,9-DMP, respectively. On the other hand, their respective fitted frequencies are 1908.0, 1916.9, and 1919.9 cm^{-1}. This band is assigned to a combination of ($\nu_{66} + \nu_{40}$) for 1,9-DMP, ($\nu_{66} + \nu_{38}$) for 2,4-DMP, and ($\nu_{65} + \nu_{39}$) for 3,9-DMP. The next band observed at 1944.8, 1943.1, and 1942.9 cm^{-1} for 1,9-, 2,4-, and 3,9-DMP, respectively, is assigned as the first overtone of ν_{40}, ν_{41}, and ν_{39} in 1,9-, 2,4-, and 3,9-DMPs, respectively.

The DFT calculated nonfundamental anharmonic band at 2078.8, 1989.0, and 2096.0 cm^{-1} is correlated with the observed ones. Another band found at 2745.5 cm^{-1} in 1,9-DMP, 2744.4 cm^{-1} in 2,4-DMP, and 2743.5 cm^{-1} in 3,9-DMP corresponds to the calculated anharmonic band at 2751.0 cm^{-1} in 1,9-DMP, 2896.6 cm^{-1} in 2,4-DMP, and 2774.7 cm^{-1} in 3,9-DMP, which is also the first overtone of ν_{24} for 1,9-DMP, ν_{21} for 2,4-DMP, and ν_{24} for 3,9-DMP, respectively. The mean deviations between observed and calculated (anharmonic or force field) nonfundamental frequencies are found to be ∼60 cm^{-1}, when the last two sets of bands are assigned as an overtone band. Therefore, alternatively we tried to assign these bands as a combination band as shown in Table 5. With this alternative assignment the mean deviation is found to be ∼10 cm^{-1} and 16−45 cm^{-1} for the scaled force field fitting method and the anharmonic calculation, respectively.

IV. CONCLUSION

We have reported the gas phase vibrational spectra of 1,9-DMP, 2,4-DMP, and 3,9-DMP at 0.5 cm^{-1} resolution and assigned the spectra using DFT calculated scaled force field frequencies and PEDs of their normal modes at the B3LYP/6-311G** level of theory. DFT calculated anharmonic frequencies are less accurate for the assignment of the aromatic C−H and methyl C−H stretching fundamentals. The error in fitting is, however, within 3 cm^{-1} between the observed fundamental vibrations and Pulay's scaled force field fitted frequencies. In fact, the exact nature of some of the vibrations in DMPs, which was wrongly assigned in phenanthrene, has been identified and corrected. In the methyl and aromatic stretching regions, the possibility of Fermi resonances appearing in the spectra could not be completely ruled out but isotopic substitution in DMPs will perhaps resolve this issue in the future.

■ ASSOCIATED CONTENT

Supporting Information. Tables listing optimized Cartesian coordinates obtained at the B3LYP/6-311G** level, internal and nonredundant local coordinates, scaled force constants in terms of NLCs, and scaling factors, calculated (harmonic, anharmonic, and force field fitted) frequencies obtained at B3LYP/6-311G** and their corresponding PEDs, observed frequencies and their intensities for DMPs. Measured and

calculated bond lengths (in Å) for phenanthrene, 4-methylphenanthrene, DMPs and atomic polar tensor (APT) charges (in electron) for phenathrene and DMPs. Tables listing the calculated intensity, observed band area, and their corresponding individual vapor pressure. This information is available free of charge via the Internet at http://pubs.acs.org.

AUTHOR INFORMATION

Corresponding Author

*E-mail: pkdas@ipc.iisc.ernet.in (P.K.D.), arunan@ipc.iisc.ernet.in (E.A.). Phone: 91-80-22932662 (P.K.D.), 91-80-22932828 (E.A.). Fax: 91-80-2360-1552.

ACKNOWLEDGMENT

The apparatus used in the experiment is supported by the FIST program of the Department of Science and Technology, Government of India. P.K.D. thanks CSIR, New Delhi, for supporting this research. We thank Prof. S. Manogaran of Department of Chemistry, Indian Institute of Technology, Kanpur, for many helpful discussions and for providing the modified UMAT program in the QCPE package.

REFERENCES

(1) Clemett, S. J.; Maechling, C. R.; Zare, R. N.; Swan, P. D.; Walker, R. M. *Science* **1993**, *262*, 721.

(2) (a) Kovalenko, L. J.; Maechling, C. R.; Clemett, S. J.; Philippoz, J. M.; Zare, R. N.; Alexander, C. M. *Anal. Chem.* **1992**, *64*, 682. (b) Elsila, J. E.; De Leon, N. P.; Buseck, P. R.; Zare, R. N. *Geochim. Cosmochim. Acta* **2005**, *69*, 1349.

(3) Fisher, S. J.; Alexander, R.; Ellis, L.; Kagi, R. I. *Polycyclic Aromat. Compd.* **1996**, *9*, 257.

(4) Zamperlini, G. C. M.; Silva, M. R. S.; Vilegas, W. *Chromatographia* **1997**, *46*, 655.

(5) Garrigues, P.; Parlanti, E.; Radke, M.; Bellocq, J.; Willsch, H.; Ewald, M. *J. Chromatogr.* **1987**, *395*, 217.

(6) Poster, D.; Lopez De Alda, M. J.; Wise, S. A.; Chuang, J. C.; Mumford, J. L. *Polycyclic Aromat. Compd.* **2000**, *20*, 79.

(7) (a) Tsapakis, M.; Stephanou, E. G. *Environ. Pollut.* **2005**, *133*, 147. (b) Lane, D. A.; Leithead, A.; Baroi, M.; Lee, J.; Graham, L. A. *Polycyclic Aromat. Compd.* **2008**, *28*, 545. (c) Filippo, P. D.; Riccardi, C.; Pomata, D.; Gariazzo, C.; Buiarelli, F. *Water Air Soil Pollut.* **2010**, *211*, 231.

(8) Orecchio, S. *J. Hazard. Mater.* **2010**, *180*, 590.

(9) Lian, J. J.; Li, C. L.; Ren, Y.; Cheng, T. T.; Chen, J. M. *Bull. Environ. Contam. Toxicol.* **2009**, *82*, 189.

(10) Pakdel, H.; Roy, C. *Energy Fuels* **1991**, *5*, 427.

(11) Cane, E.; Miani, A.; Palmieri, P.; Tarroni, R.; Trombetti, A. *J. Chem. Phys.* **1997**, *106*, 9004.

(12) Cane, E.; Miani, A.; Palmieri, P.; Tarroni, R.; Trombetti, A. *Spectrochim. Acta Part A* **1997**, *53*, 1839.

(13) (a) Pulay, P.; Fogarasi, G.; Pongor, G.; Boggs, J. E.; Vargha, A. *J. Am. Chem. Soc.* **1983**, *105*, 7037. (b) Fogarasi, G.; Pulay, P. *J. Mol. Struct.* **1986**, *141*, 145.

(14) Pirali, O.; Van-Oanh, N.-T.; Parneix, P.; Vervloet, M.; Brechignac, P. *Phys. Chem. Chem. Phys.* **2006**, *8*, 3707.

(15) Das, P.; Manogaran, S.; Arunan, E.; Das, P. K. *J. Phys. Chem. A* **2010**, *114*, 8351.

(16) Oja, V.; Suuberg, E. M. *J. Chem. Eng. Data* **1998**, *43*, 486.

(17) Calculated using Advanced Chemistry Development (ACD/Labs) Software V11.02 (1994−2011 ACD/Labs).

(18) Frisch, M. J.; Trucks, G. W.; Schlegel, H. B.; Scuseria, G. E.; Robb, M. A.; Cheeseman, J. R.; Scalmani, G.; Barone, V.; Mennucci, B.; Petersson, G. A.; Nakatsuji, H.; Caricato, M.; Li, X.; Hratchian, H. P.; Izmaylov, A. F.; Bloino, J.; Zheng, G.; Sonnenberg, J. L.; Hada, M.; Ehara, M.; Toyota, K.; Fukuda, R.; Hasegawa, J.; Ishida, M.; Nakajima, T.; Honda, Y.; Kitao, O.; Nakai, H.; Vreven, T.; Montgomery, J. A., Jr.; Peralta, J. E.; Ogliaro, F.; Bearpark, M.; Heyd, J. J.; Brothers, E.; Kudin, K. N.; Staroverov, V. N.; Kobayashi, R.; Normand, J.; Raghavachari, K.; Rendell, A.; Burant, J. C.; Iyengar, S. S.; Tomasi, J.; Cossi, M.; Rega, N.; Millam, J. M.; Klene, M.; Knox, J. E.; Cross, J. B.; Bakken, V.; Adamo, C.; Jaramillo, J.; Gomperts, R.; Stratmann, R. E.; Yazyev, O.; Austin, A. J.; Cammi, R.; Pomelli, C.; Ochterski, J. W.; Martin, R. L.; Morokuma, K.; Zakrzewski, V. G.; Voth, G. A.; Salvador, P.; Dannenberg, J. J.; Dapprich, S.; Daniels, A. D.; Farkas, O.; Foresman, J. B.; Ortiz, J. V.; Cioslowski, J.; Fox, D. J. *Gaussian 09*, Revision A.02; Gaussian, Inc.: Wallingford, CT, 2009.

(19) Rauhut, G.; Pulay, P. *J. Phys. Chem.* **1995**, *99*, 3093.

(20) Manogaran, S.; Chakraborty, D. *J. Mol. Struct. (THEOCHEM)* **1998**, *432*, 139.

(21) McIntosh, D. F.; Peterson, M. R. *UMAT, General Vibrational Analysis System, QCPE 576*; Indiana University: Bloomington, IN.

(22) Chakraborty, D.; Ambashta, R.; Manogaran, S. *J. Phys. Chem.* **1996**, *100*, 13963.

(23) Stoppa, P.; Charmet, A. P.; Tasinato, N.; Giorgianni, S.; Gambi, A. *J. Phys. Chem. A* **2009**, *113*, 1497.

(24) Galabov, B. S.; Dudev, T. Vibrational Intensities. In *Vibrational Spectra and Structure*; Durig, J. R., Ed.; Elsevier: Amsterdam, 1996; Vol. 22.

(25) Dykyj, J.; Svoboda, J.; Wilhoit, R. C.; Frenkel, M.; Hall, K. R. Vapor Pressure of Chemicals. In *Landolt-Bornstein: Numerical Data and Functional Relationships in Science and Technology*; Hall, K. R., Ed.; Springer: Berlin, 1999; Vol. 20.

(26) (a) Lavalley, J. C.; Sheppard, N. *Spectrochim. Acta* **1972**, *28A*, 2091. (b) McKean, D. C. *Spectrochim. Acta* **1973**, *29A*, 1559. (c) Daunt, S. J.; Shurvell, H. F. *Spectrochim. Acta* **1976**, *32A*, 1545. (d) Reddy, K. V.; Heller, D. F.; Berry, M. J. *J. Chem. Phys.* **1982**, *76*, 2814. (e) Cavagnat, D.; Lespade, L. *J. Chem. Phys.* **2001**, *114*, 6030. (f) Cavagnat, D.; Lespade, L. *J. Chem. Phys.* **2001**, *114*, 6041. (g) Gellini, C.; Moroni, L.; Muniz-Miranda, M. *J. Phys. Chem. A* **2002**, *106*, 10999.

(27) Semmler, J.; Yang, P. W.; Crawford, G. E. *Vibr. Spectrosc.* **1991**, *2*, 189.

(28) Trotter, J. *Acta Crystallogr.* **1963**, *16*, 605.

(29) Imashiro, F.; Saika, A.; Taira, Z. *J. Org. Chem.* **1987**, *52*, 5727.

(30) Kross, R. D.; Fassel, V. A.; Margoshes, M. *J. Am. Chem. Soc.* **1956**, *78*, 1332.